Reprinted from The Journal of Physical Chemistry, 1991, 95.

Excited States of M(II,d^6)–4′-Phenylterpyridine Complexes: Electron Localization†

Edmond Amouyal,*,‡ Mona Mouallem-Bahout,‡ and Gion Calzaferri*,§

Physico-Chimie des Rayonnements, Université de Paris-Sud, URA du CNRS No. 75, Bâtiment 350, 91405 Orsay, France, and Institute for Inorganic and Physical Chemistry, University of Bern, CH-3000 Bern 9, Switzerland *(Received: March 7, 1991)*

We report spectroscopic and photophysical data of para-substituted phenylterpyridine (ptpy) Ru(II) complexes and molecular orbital studies of the Fe(II), Ru(II), and Os(II) compounds $[M(R\text{-}ptpy)_2]^{2+}$, R = H, CH_3, OH, OCH_3, and Cl. The visible charge-transfer absorption of the $[Ru(R\text{-}ptpy)_2]^{2+}$ is almost twice as intense as observed for the corresponding 2,2′-bipyridine (bpy) complex $[Ru(bpy)_3]^{2+}$, and it is red shifted by about 50 nm. The luminescence in solution and in membranes (Nafion, cellophane) is very weak at room temperature, and the luminescence decay time is on the order of a few nanoseconds. In a glass at 77 K, however, the luminescence quantum yield is 0.4 and the decay time 13 μs. Excited-state absorption spectra measured at room temperature by laser flash spectroscopy support the interpretation that the first excited state is of the MLCT type. The similarity of the excited-state absorptions to those of the ligand radical anions strengthens the idea that the excited electron is localized on a single ligand. Molecular orbital studies indicate that the nonplanar ligand becomes planar in states corresponding to the $(n)^1(\pi^*)^1$ and the $(\pi)^1(\pi^*)^1$ excited configurations and in the MLCT state of the complex. The same holds for the ligand radical anion. Low-lying d states in the $[Fe(R\text{-}ptpy)_2]^{2+}$ complexes provide efficient relaxation channels by internal conversion. In the Ru(II) and even more pronounced in the Os(II) complexes, these states lie far above the MLCT state and can be neglected. Thus the low luminescence quantum yield at room temperature is due to low-energy intramolecular vibrations of the nonrigid complex and not to the coupling with d states. Lowering the temperature results in freezing these intramolecular movements and hence in significantly increasing the luminescence quantum yield. The molecular orbital studies indicate that it is reasonable to describe the MLCT state as $[(L)Ru^{III}(L^{\bullet-})]^{2+}$ because the perpendicular conformation of the two ligands causes all π orbitals to be accidentally 2-fold degenerate and therefore a small asymmetric distortion is sufficient to favor the localized situation.

Introduction

Polypyridine complexes of transition metals are often efficient in electron- and energy-transfer processes. They are used as photosensitizers in model systems for photochemical conversion of solar energy, and they are also considered as candidates for components in molecular electronic devices.[1,2] 2,2′-Bipyridine (bpy) complexes of Ru(II), especially $[Ru(bpy)_3]^{2+}$, have been extensively studied,[2,3] but only a few photophysical reports have been devoted to terpyridine (tpy) $[Ru(tpy)_2]^{2+}$ analogues, probably because these compounds are regarded as being nonluminescent and bearing a very short excited-state lifetime at room temperature.[4] Their structure, however, seems well adapted for constructing special devices for directed electron transfer, for photocatalysis in modified zeolites, and for photosensitization of modified electrodes.[5] We have therefore carried out experimental and theoretical studies on spectroscopic and photophysical properties of the para-substituted phenylterpyridine (ptpy) $[M(II,d^6)(R\text{-}ptpy)_2]^{2+}$ complexes **1**, M = Fe, Ru, or Os and R = H, CH_3, OH, OCH_3, or Cl. They are well suited to discuss the problem of localization versus delocalization of the promoted electron in the excited state. To understand the behavior of their

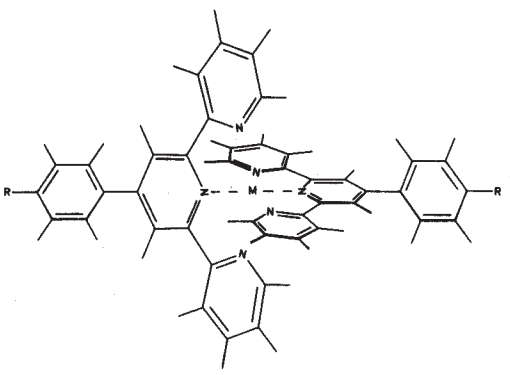

1

MLCT state, we compare the localized picture on the left side of Scheme I with the delocalized one on the right side, and we

† Part of this paper has been presented by E.A. at the XII IUPAC Symposium on Photochemistry, Bologna 1988.[1]

* Authors to whom correspondence should be addressed.

‡ URA du CNRS No. 75.

§ University of Bern.

(1) Amouyal, E.; Bahout, M.; Calzaferri, G.; Kamber, I. XII IUPAC Symposium on Photochemistry, July 17–22, Bologna, Italy, 1988, Book of Abstracts ST6, p 92.

(2) (a) Amouyal, E. *Sci. Pap. Inst. Phys. Chem. Res. (Jpn.)* **1985**, *78*, 220. (b) Rettig, W. In *Supramolecular Photochemistry*; Balzani, V., Ed.; D. Reidel Publishing Co.: Dordrecht, 1987; p 329. (c) Balzani, V.; Scandola, F. *Supramolecular Photochemistry*; Ellis Horwood: Chichester, U.K., 1990. (d) Fox, M. A., Chanon, M., Ed. *Photoinduced Electron Transfer, Part D*; Elsevier: New York, 1988. (e) Belser, P. *Chimia* **1990**, *44*, 226.

0022-3654/91/2095-7641$02.50/0

SCHEME I

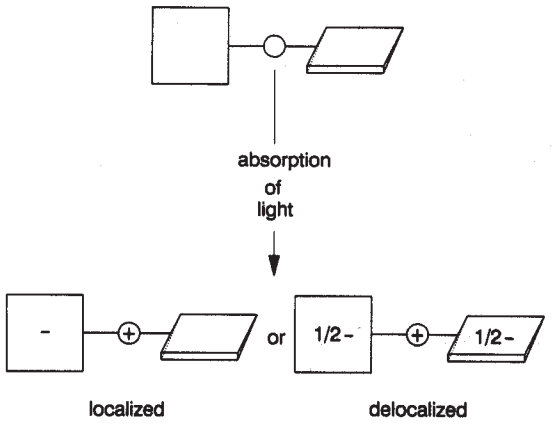

elucidate the influence of the phenyl group.

Experimental Section

Ligands and complexes with Br^- as anions have been synthesized, purified, and characterized as described in ref 6. Electronic absorption and emission spectra were measured in ethanol (Merck p.a.). ^1H NMR and IR spectra of the ligands are as reported in ref 7.

The ligand radical anions $L^{\bullet -}$ were prepared by chemical reduction of the free ligands L with solvated electrons produced by dissolution of sodium in THF under vacuum. Great care was taken to purify all chemicals. Ligands were recrystallized several times in the dark from ethanol. THF was deaerated by several freeze–pump–thaw cycles and distilled in the presence of an excess of sodium. Sodium used for the reduction was prepared in situ by thermal decomposition of NaN_3. The reaction was carried out in a special vessel sealed to a 10-mm quartz cell for spectroscopy. After reduction was completed, the resulting green solution was transferred to the quartz cell.

Laser flash spectroscopy was performed by using an excimer laser, Lambda Physik EMG 100 at 308 nm (150-mJ pulses of 10-ns duration), as an excitation source. The detection system consisted of a xenon flash lamp, a Jobin Yvon H25 monochromator, a Hamamatsu R955 photomultiplier, and a Tektronix 7904 oscilloscope. Exciting and monitoring beams were set in a 90° arrangement. The analysis was carried out within the first millimeter of the sample. In order to normalize transient optical densities, the relative laser pulse intensity was monitored by diverting a small fraction of the excimer laser beam onto a photodiode (EG & G, UV-100BQ), the output of which was displayed on a custom-built electronic integrator. Some of the experiments were made by using the 3rd harmonic (355 nm) of a pulsed Nd:YAG laser (Quantel: maximum energy 100 mJ, 3-ns pulse width) as an excitation source. The laser power was attenuated to avoid biphotonic events. Measurements were performed at room temperature. The excited-state lifetimes of the Ru^{II}ptpy complexes are of the order of the time resolution of the laser flash setups. The results have therefore been verified by single photon counting measurements using synchrotron radiation (repetition rate 13.6 MHz, pulse duration 1.3 ns) as an excitation source.[8]

TABLE I: EHMO Parameters (k = 2.0; δ = 0.35)

orbital		Slater exponent	Coulomb integral, eV
H	1s	1.3	−13.6
C	2s	1.625	−21.4
	2p	1.625	−11.4
N	2s	1.95	−26.0
	2p	1.95	−13.4
O	2s	2.275	−32.3
	2p	2.275	−14.8
Cl	3s	2.03	−30.0
	3p	2.03	−15.0
Fe	4s	1.575	−10.2
	4p	0.975	−6.72
Ru	5s	2.08	−9.23
	5p	2.04	−5.78
Os	6s	2.45	−6.55
	6p	2.37	−3.96

orbital		C_1	C_2	ζ_1	ζ_2	Coulomb integral, eV
Fe	3d	0.565	0.585	5.35	2.20	−12.27
Ru	4d	0.534	0.637	5.38	2.30	−12.14
Os	5d	0.637	0.559	5.57	2.42	−12.31

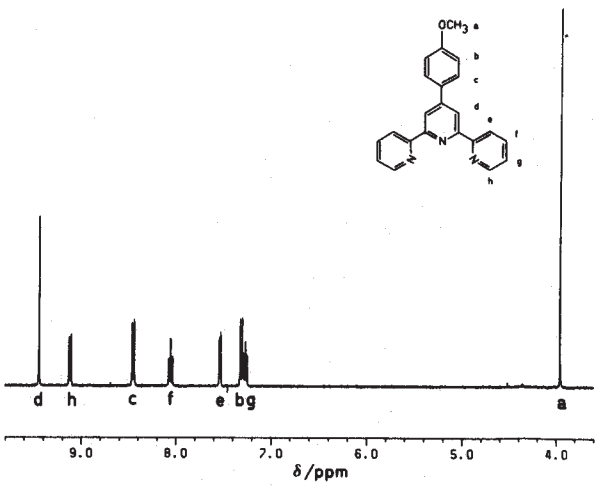

Figure 1. ^1H NMR spectrum of $[Ru(OCH_3\text{-ptpy})_2]^{2+}$ in DMSO-d_6 at room temperature. Chemical shifts (δ) in ppm, coupling constants in Hz, 3.95 (s, 6 H, H_a), 7.26 (ddd, 4 H, H_g, J_{gh} = 8, J_{gf} = 7, J_{ge} = 1), 7.31 [m(AA'BB'), 4 H, H_b], 7.53 (d, br, 4 H, H_e, J_{ef} = 5), 8.05 (ddd, 4 H, H_f, J_{fe} = 5, J_{fg} = 7, J_{fh} = 1), 8.45 [m(AA'BB'), 4 H, H_c], 9.12 (d, br, 4 H, H_h, J_{hg} = 8), 9.45 (s, 4 H, H_d).

Molecular orbital calculations have been carried out by the extended Hückel method,[9] with the parameters listed in Table I. The off-diagonal elements were calculated as[10]

$$H_{ij} = \tfrac{1}{2}kS_{ij}(H_{ii} + H_{jj}) \quad (1)$$

by using the weighted Wolfsberg–Helmholz formula[11] with a distance-dependent Hückel constant[12]

$$k = 1 + \kappa e^{-\delta(R-d_0)} \quad (2)$$

To correct for the core–core repulsion, a two-body term as ex-

(3) (a) De Armond, M. K.; Myrick, M. L. *Acc. Chem. Res.* **1989**, *22*, 364. (b) Juris, A.; Barigeletti, F.; Campagna, S.; Balzani, V.; Belser, P.; von Zelewsky, A. *Coord. Chem. Rev.* **1988**, *84*, 85. (c) Meyer, T. J. *Pure Appl. Chem.* **1990**, *62*, 1003. Ibid. **1986**, *58*, 1193.

(4) (a) Winkler, J. R.; Netzel, T. L.; Creutz, C.; Sutin, N. *J. Am. Chem. Soc.* **1987**, *109*, 2381. (b) Kirchhoff, J. R.; McMillin, D. R.; Marnot, P. A.; Sauvage, J.-P. *J. Am. Chem. Soc.* **1985**, *107*, 1138. (c) Stone, M. L.; Crosby, G. A. *Chem. Phys. Lett.* **1981**, *79*, 169. (d) Agnew, S. F.; Stone, M. L.; Crosby, G. A. *Chem. Phys. Lett.* **1982**, *85*, 57. (e) Braterman, P. S. *Chem. Phys. Lett.* **1984**, *104*, 405. (f) Demas, J. N.; Crosby, G. A. *J. Am. Chem. Soc.* **1971**, *93*, 2841.

(5) (a) Calzaferri, G. *Chimia* **1986**, *40*, 74. (b) Calzaferri, G.; Gori, M.; Grüniger, H. R.; Spahni, W. *Proceedings Photoelectrochemistry: Fundamental Processes and Measurement Techniques, The Electrochemical Soc.*; Wallace, W. L., Nozik, A. J., Deb, S. K., Wilson, R. H., Eds.; 1982, Vol. 82-3, p 264. (c) Beer, R.; Calzaferri, G.; Gfeller, N.; Li, J.; Waldeck, B. *Proceedings, SPSE, 44*, 1991, in press.

(6) Spahni, W.; Calzaferri, G. *Helv. Chim. Acta* **1984**, *67*, 450.

(7) Sadtler *Handbook of Proton NMR Spectra, Sadtler Research Laboratories, Philadelphia, USA*, 1987, and Sadtler *Handbook of Infrared Spectra, Sadtler Research Laboratories, Philadelphia, USA*, 1987.

(8) Royer, C. A.; Tauc, P.; Hervé, G.; Brochon, J.-C. *Biochemistry* **1987**, *26*, 6472.

(9) Hoffmann, R. *J. Chem. Phys.* **1963**, *39*, 1397.

(10) Wolfsberg, M.; Helmholz, L. *J. Chem. Phys.* **1952**, *20*, 837.

(11) Ammeter, J. H.; Bürgi, H.-B.; Thibeault, J. C.; Hoffmann, R. *J. Am. Chem. Soc.* **1978**, *100*, 3686.

(12) (a) Calzaferri, G.; Hoffmann, R. *J. Chem. Soc., Dalton Trans.* **1991**, 917. (b) Calzaferri, G.; Forss, L.; Kamber, I. *J. Phys. Chem.* **1989**, *93*, 5366.

TABLE II: Data on Electronic Absorption Spectra in Ethanol

compound	visible		UV					
	λ_{max}, nm	ϵ_{max}, M^{-1} cm^{-1}	λ_{max}, nm	ϵ_{max}, M^{-1} cm^{-1}	λ_{max}, nm	ϵ_{max}, M^{-1} cm^{-1}	λ_{max}, nm	ϵ_{max}, M^{-1} cm^{-1}
$[Ru(bpy)_3]^{2+}\cdot 2Cl^-$	445	14 500			285	88 500	242	30 300
$[Ru(tpy)_2]^{2+}\cdot 2PF_6^-$	473	16 100	306	72 300	270	48 000		
$[Ru(Cl\text{-}ptpy)_2]^{2+}\cdot 2Br^-$	490	24 600	310	60 600	283	56 300		
$[Ru(CH_3\text{-}ptpy)_2]^{2+}\cdot 2Br^-$	488	26 400	307	66 500	283	56 900		
$[Ru(OH\text{-}ptpy)_2]^{2+}\cdot 2Br^-$	496	26 100	306	95 900	284	97 500		
$[Ru(OCH_3\text{-}ptpy)_2]^{2+}\cdot 2Br^-$	495	24 400	308	60 500	283	48 900		
$[Fe(OCH_3\text{-}ptpy)_2]^{2+}\cdot 2Br^-$	570	25 000	325		280			
OCH_3-ptpy					282	39 700		

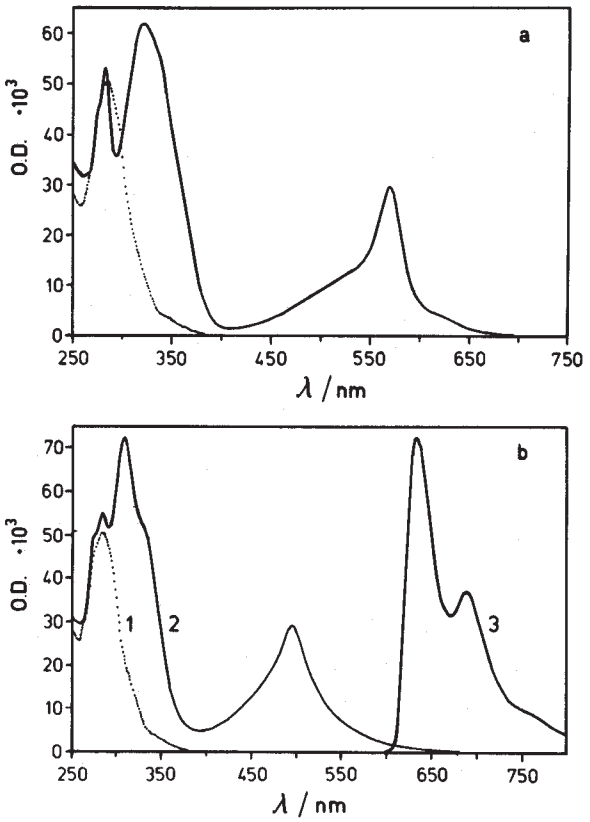

Figure 2. (a) Absorption spectra of the ligand (dotted curve) and of $[Fe(OCH_3\text{-}ptpy)_2]^{2+}$ (solid curve) in 10^{-5} M ethanol solutions at room temperature. (b) Absorption spectrum of the ligand (1) and absorption spectrum of the $[Ru(OCH_3\text{-}ptpy)_2]^{2+}$ complex (2) in 10^{-5} M ethanol solution at room temperature and the corrected emission spectrum (3) of this complex in 10^{-3} M ethanol glass at 77 K. The intensity of the emission spectrum is in arbitrary units.

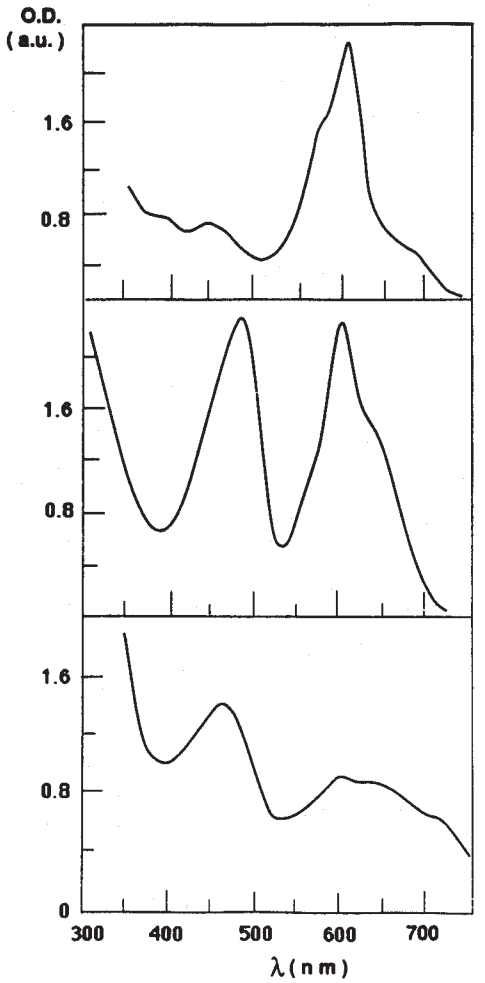

Figure 3. Absorption spectra of the ligand radical anions in THF: top, $tpy^{\bullet -}$; middle, $Cl\text{-}ptpy^{\bullet -}$; bottom, $OCH_3\text{-}ptpy^{\bullet -}$.

plained in refs 12 and 13 has been taken into account. Bond lengths have been chosen as follows: C–H, 1.08 Å; C–C aromatic, 1.4 Å; C–N, 1.35 Å; C–C phenyl–phenyl, 1.49 Å; C–Cl, 2.0 Å. If not stated otherwise, results obtained for the planar conformation of the ligands and for a metal–nitrogen distance of 2 Å are reported.

Results

The ^1H NMR spectrum of $[Ru(OCH_3\text{-}ptpy)_2]^{2+}$ presented in Figure 1 demonstrates the high symmetry of the complex, and it shows that given the time resolution of the technique, both ligands are geometrically equivalent, notably the terminal pyridine groups. The ^1H NMR spectra of the other complexes look similar and sustain this interpretation.

Ground-State Absorption. The electronic absorption spectra of $[Fe(OCH_3\text{-}ptpy)_2]^{2+}$ and of $[Ru(OCH_3\text{-}ptpy)_2]^{2+}$ shown in Figure 2 look very similar. The visible part of these spectra consists of at least three bands, and in the near-UV region two main absorptions can be distinguished. The long-wavelength tail of the spectra extends to nearly 700 nm. The maximum of the visible band of the nonluminescent Fe(II) complex is red shifted by about 75 nm with respect to the Ru(II) analogue, and so is the second strong absorption in the near-UV. The maximum at 280 nm coincides with the $\pi^* \leftarrow \pi$ transition of the free ligand. We have observed that the absorption spectra of the $[Ru(R\text{-}ptpy)_2]^{2+}$ complexes are only moderately influenced by the substituent R as documented in Table II. They are all similar to the one shown in Figure 2b. Let us notice that the visible band of the $[Ru(R\text{-}ptpy)_2]^{2+}$ attributed to a MCLT transition is red shifted up to 50 nm with respect to $[Ru(bpy)_3]^{2+}$ and that the corresponding extinction coefficients are about 2 times larger.

The electronic absorption spectra of the ligand radical anions in Figure 3, however, show significant dependence on R. The visible spectrum of $Cl\text{-}ptpy^{\bullet -}$ exhibits two bands of the same intensity with maxima at 485 and 600 nm and a shoulder at about 640 nm. Two broader bands of differing intensity with maxima at 465 and 605 nm and two shoulders at 640 and 715 nm are observed for $OCH_3\text{-}ptpy^{\bullet -}$. The radical anion $tpy^{\bullet -}$ exhibits two bands in the visible region with maxima at 445 and 610 nm and shoulders at 580 and 675 nm, among other features. The 610-nm absorption is very intense. Our results are in agreement with the

(13) Anderson, A. B.; Hoffmann, R. *J. Chem. Phys.* **1974**, *60*, 4271.

TABLE III: Data on Emission Spectra in Ethanol

compound	solvent	293 K λ_{max}, nm	293 K ϕ_E	293 K τ, ns	77 K λ_{max}, nm	77 K ϕ_E	77 K τ, μs
$[Ru(bpy)_3]^{2+}\cdot 2Cl^-$	ethanol	610	0.042[b]	1330	580, 630, 680[a]	0.38[a]	5.2[a]
$[Ru(Cl\text{-}ptpy)_2]^{2+}\cdot 2Br^-$	ethanol	645	0.00004	11			
$[Ru(OCH_3\text{-}ptpy)_2]^{2+}\cdot 2Br^-$	ethanol	650	0.00003	4.8	632, 690, 745	0.4	13
$[Ru(OCH_3\text{-}ptpy)_2]^{2+}\cdot 2Br^-$	Nafion	610, 680	0.0004	10			
$[Ru(CH_3\text{-}ptpy)_2]^{2+}\cdot 2Br^-$	ethanol	640	0.00001	4.5			

[a] In ethanol–methanol mixture.[4e,36] [b] In water.[37]

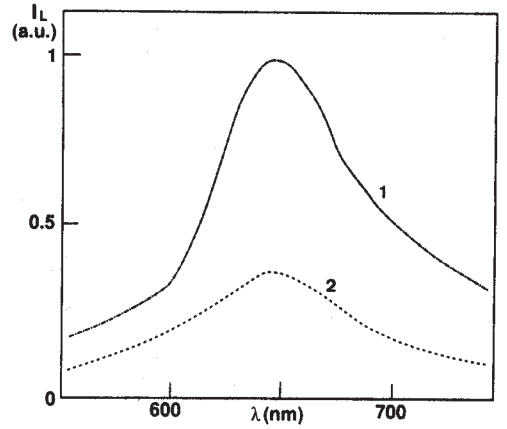

Figure 4. Room temperature luminescence spectra (not corrected) of a 7.3×10^{-5} M $[Ru(OCH_3\text{-}ptpy)_2]^{2+}$ (1) and of a 4.0×10^{-5} M $[Ru(Cl\text{-}ptpy)_2]^{2+}$ (2) solution in ethanol.

observations of Nakamura,[14] who reported part of this spectrum in 1971.

Emission. No luminescence has been detected for $[Fe(OCH_3\text{-}ptpy)_2]^{2+}$. The corrected emission spectrum of $[Ru(OCH_3\text{-}ptpy)_2]^{2+}$ measured at 77 K is shown in Figure 2b, and in Table III we give the position of the emission maximum, the quantum yield, and the lifetime at 77 K, and we compare these data with those of $[Ru(bpy)_3]^{2+}$. The luminescence spectrum of $[Ru(OCH_3\text{-}ptpy)_2]^{2+}$ looks similar to that of the bpy complex. It is, however, red shifted by about 40 nm. The quantum yield is nearly the same as this temperature, and the emission lifetime of 13 μs is twice as high as that of $[Ru(bpy)_3]^{2+}$. By analogy with the latter compound, the emission is readily assigned to a d $\leftarrow$ π^* transition. To our knowledge, no room temperature emission spectrum of a $[Ru(R\text{-}ptpy)_2]^{2+}$ or a $[Ru(tpy)_2]^{2+}$ complex has been reported. We therefore show in Figure 4 the uncorrected steady-state room temperature emission spectra of the methoxy and of the chloro derivatives in ethanol solutions. We have checked that the very weak emissions are not due to impurities from the solvent or from the free ligand. The room temperature quantum yields are 3 orders of magnitude lower than that of $[Ru(bpy)_3]^{2+}$, Table III. The positions of the maxima at about 645 nm are red shifted with respect to the $[Ru(bpy)_3]^{2+}$ luminescence by 40 nm. We attribute these room temperature luminescence to the same transition as observed at 77 K. The time-resolved emission spectra of $[Ru(OCH_3\text{-}ptpy)_2]^{2+}$ and of $[Ru(Cl\text{-}ptpy)_2]^{2+}$ recorded in glycerol after excitation at 308 nm with a laser pulse are similar to the steady-state emission with $\lambda_{exc} = 495$ nm. The lifetimes for these emissions are similar to those observed for the complexes adsorbed on membranes such as Nafion or cellophane.

From the much shorter room temperature luminescence lifetimes of tpy complexes in solution with respect to that of $[Ru(bpy)_3]^{2+}$, it follows that an efficient nonradiative deactivation channel exists. A possible explanation of this fact would be deactivation via a low-lying d state, as has been proposed to explain the behavior of $[Ru(dptpy)_2]^{2+}$ (dptpy = 6,6″-diphenyl-2,2′:6′,2″-terpyridine).[4b] We are unable to explain the pronounced temperature dependence of the luminescence quantum yield observed by us on this basis. It is, however, adequate for explaining the total lack of luminescence in the case of the Fe complexes.

(14) Nakamura, K. *Bull. Chem. Soc. Jpn.* **1971**, *45*, 1943.

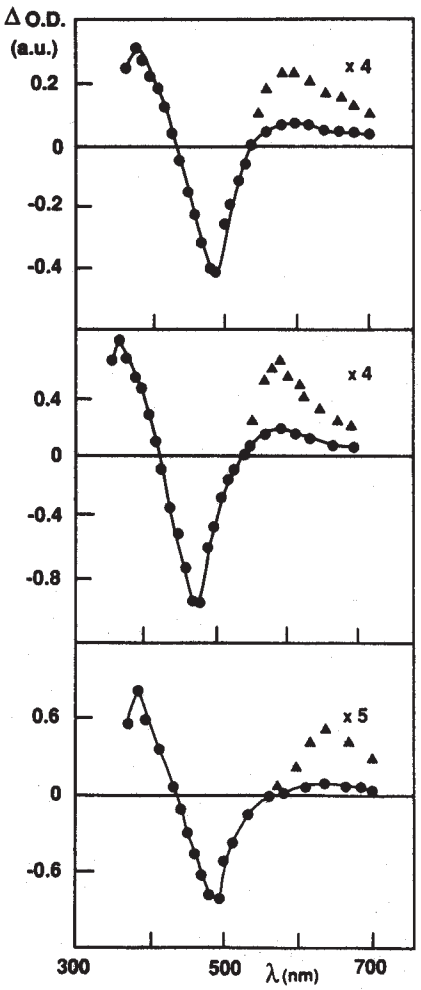

Figure 5. Differential excited-state absorption spectrum of $(3\text{–}5) \times 10^{-5}$ M solutions in ethanol, observed immediately after the end of a 308-nm laser pulse: top, $[Ru(CH_3\text{-}ptpy)_2]^{2+}$; middle, $[Ru(Cl\text{-}ptpy)_2]^{2+}$; bottom, $[Ru(OCH_3\text{-}ptpy)_2]^{2+}$.

More probably, the deactivation channel is inherent to the structure of tpy complexes, which is less rigid than that of the $[Ru(bpy)_3]^{2+}$. Efficient deactivation channels due to nonrigidity of the structures are well established in organic $\pi \leftarrow \pi^*$ luminescence.[15]

Excited-State Absorption. We have been able to measure the excited-state absorption spectra of ptpy complexes by nanosecond laser flash spectroscopy despite their very short luminescence lifetime at room temperature. Differential absorption spectra are shown in Figure 5. At shorter wavelengths than 550 nm they are comparable to those observed on various bpy complexes of Ru(II).[16] In particular, they show a negative band with a

(15) (a) Bergamasco, S.; Calzaferri, G.; Hädener, K. *J. Photochem. Photobiol. A* **1990**, *53*, 109. (b) Güsten, H.; Meisner, R. *J. Photochem.* **1983**, *21*, 53. (c) Janssen, J.; Lüttke, W. *J. Mol. Struct.* **1982**, *81*, 207. (d) Calzaferri, G.; Gugger, H. *Helv. Chim. Acta* **1976**, *59*, 1969.

(16) (a) Kumar, C. V.; Barton, J. K.; Turro, N. J.; Gould, I. R. *Inorg. Chem.* **1987**, *26*, 1455. (b) Creutz, C.; Chou, M.; Netzel, T. L.; Okumura, M.; Sutin, N. *J. Am. Chem. Soc.* **1980**, *102*, 1309. (c) Bensasson, R.; Salet, C.; Balzani, V. *J. Am. Chem. Soc.* **1976**, *98*, 3722.

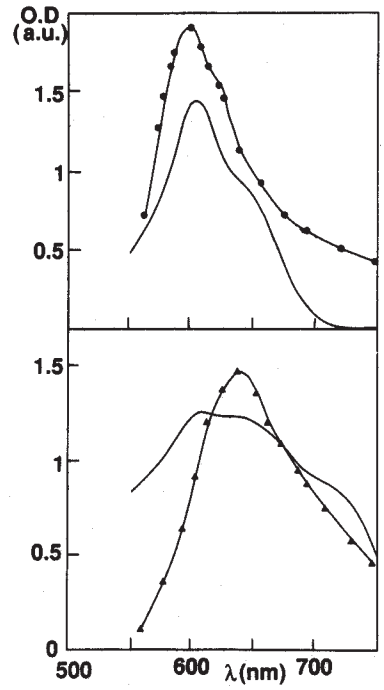

Figure 6. Comparison of the absorption spectra of the ligand anions (solid curve) with the transient absorption of the corresponding Ru(II) complex (solid curves with dots and triangles, respectively): top, Cl-ptpy; bottom, OCH_3-ptpy.

maximum at 490 nm that corresponds to the depopulation of the ground state. A new band appears above 550 nm with a maximum at 600 nm in case of $[Ru(Cl\text{-}ptpy)_2]^{2+}$. The methoxy and the methyl derivatives exhibit somewhat broader bands with maxima at 640 and 590 nm, respectively. Within the accuracy of our data, the room temperature transient absorption decay shows wavelength-independent lifetimes of 5–10 ns. For each compound these lifetimes are similar to the emission lifetimes observed under the same conditions. It is now interesting to compare in Figure 6 the spectra of the ligand radical anions $L^{\bullet -}$ with the excited-state absorption spectra of the complexes. The excited-state absorption spectra and the spectra of the ligand radical anion should be similar in the case that the MLCT state of the complex can be described as $[(R\text{-}ptpy)Ru^{III}(R\text{-}ptpy^{\bullet -})]^{2+}$. For the chloro compound the similarity of the two spectra is surprisingly good, and it is reasonable for the methoxy complex. Woodruff and co-workers[17] as well as Forster and Hester[18] established the remarkable fact that the lowest MLCT state of $[Ru(bpy)_3]^{2+}$ in aqueous solution at room temperature can be characterized as $[(bpy)_2Ru(III)(bpy^{\bullet -})]^{2+}$.[3a,16b] In approximate terms, localization occurs if the vibrational and solvation energy released is significantly larger than the electron exchange energy between ligands. There are reports that localization in this complex does not occur in a frozen, rigid environment,[19] suggesting that it requires significant excited-state solvent reorganization.[20] The situation is less clear for $[Ru(tpy)_2]^{2+}$. A very weak structureless excited-state absorption only has been reported[4a] above 550 nm which cannot be easily correlated with the visible part of the $tpy^{\bullet -}$ spectrum shown in Figure 3. On the basis of emission polarization it was argued, however, that the electron is localized on one ligand in the excited state of Ru(II) complexes containing tridentate N-heterocyclic ligands such as tpy.[4d]

(17) (a) Bradley, P. G.; Kress, N.; Hornberger, B. A.; Dallinger, R. F.; Woodruff, W. H. *J. Am. Chem. Soc.* **1981**, *103*, 7441. (b) Dallinger, R. G.; Woodruff, W. H. *J. Am. Chem. Soc.* **1979**, *101*, 4391.

(18) Forster, M.; Hester, R. E. *Chem. Phys. Lett.* **1981**, *81*, 42.

(19) (a) Kitamura, N.; Kim, H. B.; Kawanishi, Y.; Obata, R.; Tazuke, S. *J. Phys. Chem.* **1986**, *90*, 1488. (b) Krausz, E. R. *Chem. Phys. Lett.* **1985**, *116*, 501. (c) Ferguson, J.; Krausz, E. R.; Maeder, M. *J. Phys. Chem.* **1985**, *89*, 1852.

(20) Carroll, P. J.; Brus, L. E. *J. Am. Chem. Soc.* **1987**, *109*, 7613.

SCHEME II

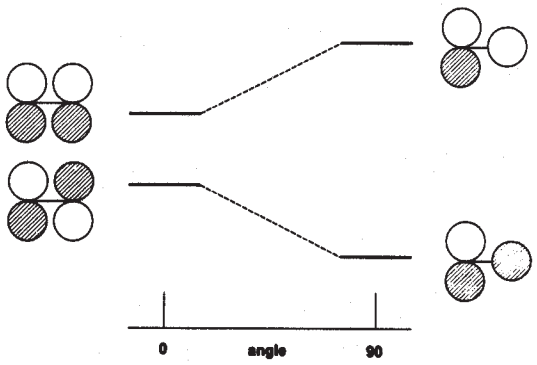

Theoretical Considerations

We now look into the electronic structure of the ligands and of the complexes in order to understand the influence of the phenyl group and its substituents on the electronic absorption spectra of the ligands and of the complexes, and we then explain the effect of the central metal on the excited-state behavior of the complexes. We first discuss the absorption spectra of the ligands L (**2**) and

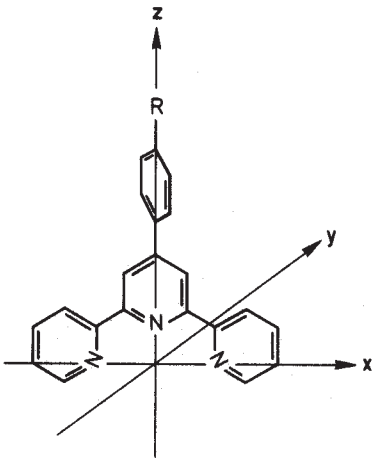

2

of the ligand radical anions $L^{\bullet -}$ and then compare them with the absorption spectra of the MLCT state of the complexes. This leads to the intriguing question of delocalization, $[Ru^{III}(L_2)^{\bullet -}]^{2+}$, versus localization, $[(L)Ru^{III}(L^{\bullet -})]^{2+}$, of the electron in the MLCT state which we raised in Scheme I.

As in bpy and tpy, the ligand **2** is not planar in the electronic ground state. The twist angle of the phenyl and the pyridine rings is of the order of 30°. Nevertheless, we present the theoretical results within the C_{2v} point group. This allows a simplified discussion without loss of important information. The relevant frontier orbitals of **2** are shown in Figure 7a. The three highest occupied orbitals of the ptpy are the lone pairs 1n, 2n, and 3n. The lowest unoccupied orbitals are of π^* type. We conclude that the first electronic transition is of the $\pi^* \leftarrow$ n type, namely, $1\pi^*(B_2) \leftarrow 1n(A_1)$, and that it is polarized vertically with respect to the π system and therefore of low intensity. The resulting state is of B_2 symmetry and corresponds to the long-wavelength tail of the ligand spectra shown in Figure 2. The $\pi^* \leftarrow$ n transitions in the tpy molecule have been studied by Fink and Ohnesorge.[21] These authors have observed the solvent dependence of the absorption spectra as typically expected for this type of transition. The absorption starts at about 420 nm in cyclohexane and nearly disappears below the $\pi^* \leftarrow \pi$ band in chloroform. The next allowed transitions are of the $\pi^* \leftarrow \pi$ type. They lead to a B_1 state in case of the x-polarized $1\pi^*(B_2) \leftarrow 1\pi(A_2)$ transition and to A_1 states for the $2\pi^*(A_2) \leftarrow 1\pi(A_2)$ and $1\pi^*(B_2) \leftarrow 2\pi(B_2)$ transitions, polarized along the z axis. We have checked the

(21) Fink, D. W.; Ohnesorge, W. E. *J. Phys. Chem.* **1970**, *74*, 72.

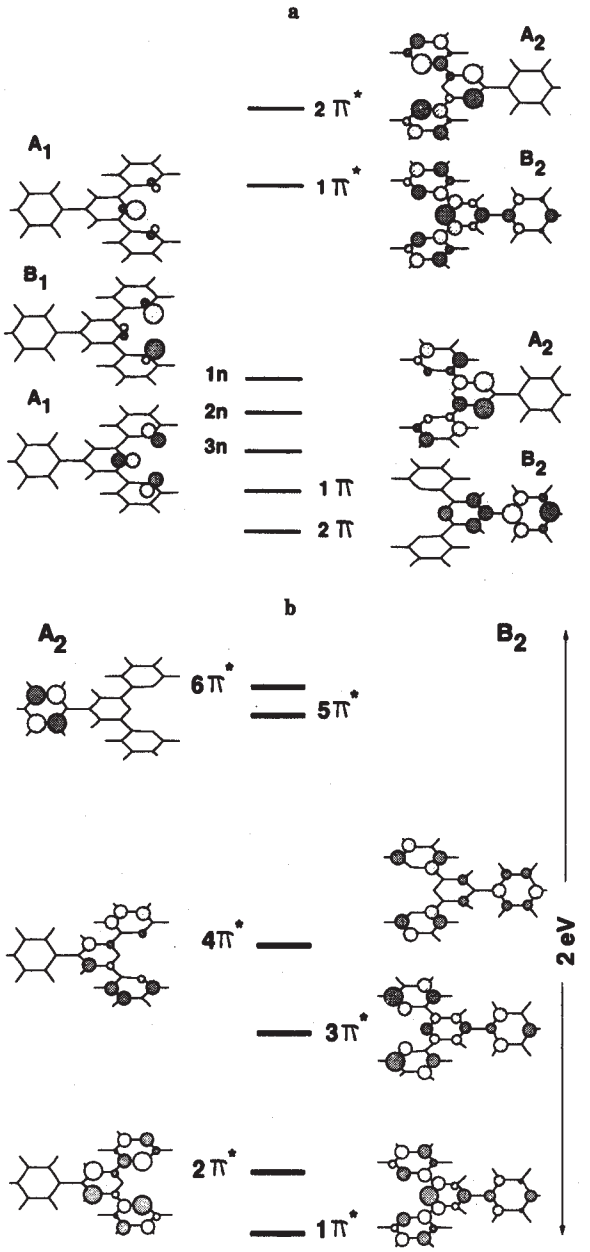

Figure 7. (a) Molecular orbital diagram of the ptpy ligand. The highest occupied orbital in the ground state is the $1n(A_1)$ lone pair. The calculated orbital energies in eV are as follows: −13.0, $2\pi(B_2)$; −12.75, $2\pi(A_2)$; −12.65, $3n(A_1)$; −12.4, $2n(B_1)$, −12.1, $1n(A_1)$; −9.25, $1\pi^*(B_2)$; and −9.0, $2\pi^*(A_2)$. (b) π^* orbitals of the ligand anion $ptpy^{\bullet -}$.

influence of configuration interaction by carrying out Pariser–Parr–Pople (PPP) calculations.[22] The main result of our PPP-CI studies is the finding that the single configuration $(1\pi A_2)^1(1\pi^*B_2)^1$ is adequate and sufficient for the description of the first excited $\pi\pi^*$ state of B_1 symmetry. To discuss the geometry of the molecule in the excited state, we have to look at the orbitals involved. The situation is similar to the one observed in the well-studied biphenyl molecule and can be rationalized by Scheme II.[15c,d] The antibonding orbital is occupied by two electrons in the ground state. The molecule therefore has a tendency to twist out of plane. In the excited state one of these antibonding electrons is promoted to the bonding orbital; hence the planar geometry is stabilized. The extended Hückel calculations (Figure 8) lead to the result that in the electronic ground state the phenyl and the pyridine rings are out of plane by an angle of about 30° while in the $(1n)^1(1\pi^*)^1$ and in the $(1\pi)^1(1\pi^*)^1$ configurations an energy minimum is found for the planar geometry. To summarize, the bonding interaction in the $1\pi^*(B_2)$ orbital between the rings is

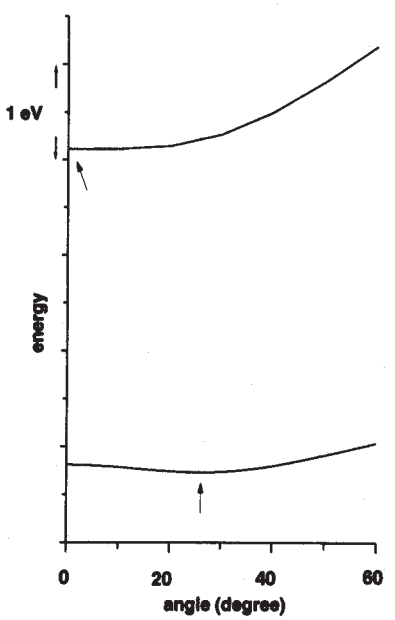

Figure 8. Energy of the electronic ground-state configuration and of the first excited $\pi\pi^*$-state configuration versus the out of plane angle of the pyridine and the phenyl groups in degrees. The energy minima are indicated by arrows.

the reason why the ligand has a tendency to become planar, and conjugation with the phenyl group is enhanced as soon as we promote an electron in this orbital. By the same arguments we predict that the ligand anion $L^{\bullet -}$ is planar.

We now discuss the influence of a substituent in the para position of the phenyl ring by applying a first-order perturbation procedure. Within this approximation, the unperturbed orbital energy $\epsilon^0_{\pi_i}$ of an orbital π_i is influenced by a substituent R as follows:

$$\epsilon_{\pi_i}(R) = \epsilon^0_{\pi_i} + c_{C,\pi_i}{}^2(\delta\alpha_R) \qquad (3)$$

c_{C,π_i} is the MO coefficient of the carbon atom adjacent to R in the π_i orbital and $\delta\alpha_R$ is the change of the Coulomb integral of the carbon atom with respect to R = H. The energy of the charge-transfer transition can therefore be written as:[23]

$$\Delta E^0_{CT}(R) = \Delta E^0_{CT} + c_{C,\pi^*_i}{}^2(\delta\alpha_R) \qquad (4)$$

We conclude that only those orbitals are influenced by a substituent R which have a nonzero coefficient on the adjacent carbon atom. Figure 7 shows that only orbitals of B_2 symmetry have nonzero coefficient c_{C,π_i}. This means that the B_2 orbitals are influenced by R while the A_2 orbitals remain unchanged. $\delta\alpha_R$ is zero for R = H and increases in the order $\delta\alpha_H < \delta\alpha_{CH_3} < \delta\alpha_{OCH_3} < \delta\alpha_{Cl}$. As long as the molecule is in the electronic ground state, it is not planar and $c_{C,\pi^*(B_2)}{}^2$ is relatively small. We therefore expect a minor influence of R on the absorption spectra of the ligands. In the excited state, however, the ligand becomes planar and this causes an increase of $c_{C,\pi^*(B_2)}{}^2$ and enhanced conjugation. As a consequence, the influence of R on the emission spectrum is more pronounced. It becomes definitely important in case of the ligand anion $L^{\bullet -}$. To understand this, we have to study the π^* orbitals shown in Figure 7b. From this figure it follows that a description of the electronic absorption spectrum of $L^{\bullet -}$ is not easy. Both the $B_2 \leftarrow B_2$ and the $A_2 \leftarrow A_2$ promotions are allowed along the z axis and lead to states of A_1 symmetry. The $A_2 \leftarrow B_2$ promotions are allowed in the x direction and result in states of B_1 symmetry. Several electronic configurations of A_1 symmetry lie within a small energy interval; configuration interaction, therefore, cannot be neglected. We also expect the solvent to have significant influence on the absorption spectra of $L^{\bullet -}$. These complications do not allow a detailed interpretation. Despite this we can conclude that $L^{\bullet -}$

(22) Mataga, N.; Nishimoto, K. *Z. Phys. Chem. NF* **1957**, *13*, 140.

(23) Calzaferri, G.; Felix, F. *Helv. Chim. Acta* **1977**, *60*, 730.

TABLE IV: Group Overlap Integrals

	G_{z^2}	$G_{x^2-y^2}$
Fe	0.13	0.10
Ru	0.19	0.16
Os	0.22	0.19

must be an intensely colored species with a spectrum extending to the near-infrared. The energy of those states in which orbitals of $\pi^*(B_2)$ are involved depends significantly on R, because c_{C,π_i}^2 is quite large, while states in which only $\pi^*(A_2)$ orbitals are involved do not depend on R because c_{C,π_i}^2 is zero.

Having understood some main features of the electronic structure of the ligand and of the ligand anions, we are prepared to study its interaction with the d^6 transition-metal cations $Fe^{2+}(3d^6)$, $Ru^{2+}(4d^6)$, and $Os^{2+}(5d^6)$. The question immediately arises, why the Ru^{2+} and the Os^{2+} complexes do show luminescence, while the Fe^{2+} complexes do not? It seems that the answer to this question is relatively simple. In Figure 10 we compare the one electron levels of the $[M^{II}(H\text{-ptpy})_2]^{2+}$ complexes. The highest occupied orbitals of the iron complex are the degenerate d_{xz} and d_{yz} followed by d_{xy}. Thus the first intense electronic transition is the $\pi^* \leftarrow$ d MLCT. The d_{z^2} and the $d_{x^2-y^2}$ orbitals are of about the same energy as the $1\pi^*$ level. We therefore expect to find d states at about the same energy as the MLCT state, and as a consequence mixing between these states occurs.[5a] According to present knowledge such mixing always leads to efficient radiationless deactivation channels because of their ability to couple strongly to vibrational modes. While intramolecular movements can be frozen by lowering the temperature,[15] this coupling cannot. It is therefore not astonishing that no luminescence of the $[Fe(R\text{-ptpy})_2]^{2+}$ complexes has been observed.

If our explanation is correct, we must expect that the d_{z^2} and the $d_{x^2-y^2}$ levels are shifted to higher energy with respect to the lowest π^* orbitals in the case of the Ru^{2+} and of the Os^{2+} complexes. Exploring this idea, we enumerate the ligands as L_1 and L_2 and take into account that they are perpendicular to each other and that the symmetry of the d_{z^2} and the $d_{x^2-y^2}$ atomic orbitals of the central atom is A_1. As a consequence, d_{z^2} and $d_{x^2-y^2}$ can only interact with the totally symmetric linear combinations

$$1n^+ = \frac{1}{2^{1/2}}(1n_{L_1} + 1n_{L_2}) \qquad 3n^+ = \frac{1}{2^{1/2}}(3n_{L_1} + 3n_{L_2}) \tag{5}$$

of the lone pair orbitals 1n and 3n illustrated in Figure 7. From this we get

$$\Psi^{\pm}(d_{z^2}) = \frac{1}{N_{z^2}{}^{1/2}}(d_{z^2} \pm 1n^+)$$
$$\Psi^{\pm}(d_{x^2-y^2}) = \frac{1}{N_{x^2-y^2}{}^{1/2}}(d_{x^2-y^2} \pm 3n^+) \tag{6}$$

The antibonding combination is of greater interest than the bonding one since it corresponds to the so called d_{z^2} and the $d_{x^2-y^2}$ levels in the energy region of the LUMO in Figure 11. To estimate the dependence of the energy of these levels on the central atom, it is convenient to make use of the concept of group overlap integrals[24] G, in our case G_{z^2} and $G_{x^2-y^2}$. They can be expressed as

$$G_{z^2} = \langle d_{z^2}|1n^+\rangle \qquad G_{x^2-y^2} = \langle d_{x^2-y^2}|3n^+\rangle \tag{7}$$

To calculate the numerical values of the group overlap integrals in Table IV, we have used the extended Hückel procedure. As in previous studies we define the relative Coulomb integral α_{rel} as[5a,25]

$$\alpha_{rel} = \alpha_d/|\alpha_L| \tag{8}$$

α_d is the Coulomb integral of the metal d orbitals, and α_L is the Coulomb integral of the envisaged ligand orbital. Applying the Wolfsberg–Helmholz formula, we get

$$\beta_{rel} = \frac{1}{2}k(\alpha_{rel} - 1)G_{dL}, \qquad G_{dL} = G_{z^2} \text{ and } G_{x^2-y^2} \tag{9}$$

The same reasoning as used in earlier studies leads to[5a,25]

$$\epsilon_{rel}^{\pm} = \frac{\alpha_{rel} - 1 - 2\beta_{rel}G_{dL}}{2(1 - G_{dL}^2)} \times \left[1 + \left\{1 + 4(1 - G_{dL}{}^2)\frac{\alpha_{rel} + \beta_{rel}{}^2}{(\alpha_{rel} - 1 - 2\beta_{rel}G_{dL})^2}\right\}^{1/2}\right] \tag{10}$$

From this we derive very general conclusions which do not depend on parametrization. In Figure 9 we show the orbital energies ϵ_{rel}^+ and ϵ_{rel}^- for $\alpha_{rel} = -1$, -0.6, and -0.2 versus the group overlap integral. ϵ^- corresponds to the energy of the so-called d_{z^2} in the case of $G_{dL} = G_{z^2}$ and to the energy of $d_{x^2-y^2}$ in the case of $G_{dL} = G_{x^2-y^2}$. To study the interaction of the d orbitals with the 1n and the 3n orbitals, a value of α_{rel} close to -1 is most relevant in the present case because the interacting ligand and metal orbitals are of approximately the same energy. It is therefore sufficient to look at the curve that starts at $(\epsilon_{rel}, G_{dL}) = (-1,0)$ and reaches (0.7,0.25) (Figure 9). The intersection of this curve with the values of $G_{x^2-y^2}$ and the values of G_{z^2} for Fe^{2+}, Ru^{2+}, and Os^{2+} (Table IV) is indicated by vertical lines. From this it is obvious that the d_{z^2} and the $d_{x^2-y^2}$ orbitals shift to much higher energy for Ru^{2+} and for Os^{2+} with respect to Fe^{2+}. This is a consequence of the fact that the atomic orbitals of Ru^{2+} and Os^{2+} extend further into space and allow much better overlap with the nitrogen lone pairs 1n and 3n. This means that for the Ru^{2+} and for the Os^{2+} complexes the d_{z^2} and the $d_{x^2-y^2}$ orbitals lie well above the $1\pi^+$ and the $2\pi^+$ levels and that therefore mixing of d states with the MLCT state can be neglected. Full extended Hückel calculations on these complexes confirm these results; see Figure 10. We can therefore understand, on a simple basis, why the iron complexes do not show luminescence at all while the ruthenium and the osmium complexes do.

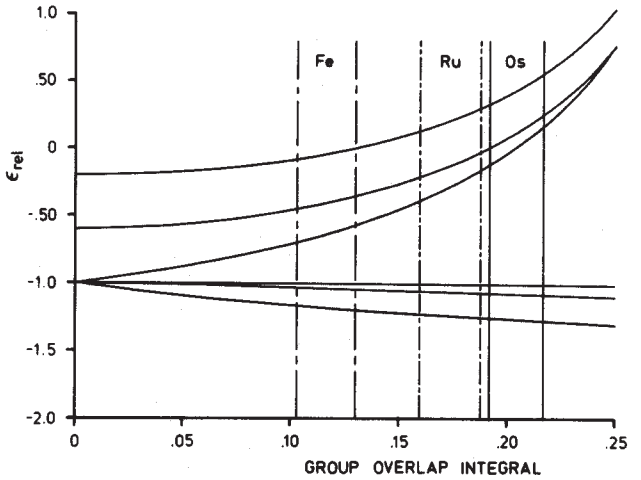

Figure 9. Orbital energies ϵ_{rel}^+ and ϵ_{rel}^- for $\alpha_{rel} = -1$, -0.6, and -0.2 versus the group overlap integral. Values of $G_{x^2-y^2}$ and G_{z^2} (Table IV) for each central atom are indicated by vertical lines. The three curves ϵ_{rel}^- all start at -1 on the left side while the three ϵ_{rel}^+ curves start at α_{rel}; this means at -1, -0.6, and -0.2, respectively.

We now give a more detailed interpretation of the electronic spectra of the $[Ru(R\text{-ptpy})_2]^{2+}$ by comparing the one-electron levels of the R-ptpy ligand with those of the complex on the right side in Figure 11. The $\pi^* \leftarrow$ n and the $\pi^* \leftarrow \pi$ transitions of the ligand have already been discussed. In the complex several new transitions can be identified. It is obvious that a very detailed analysis, in which spin–orbit interaction would have to be included, is complicated. Being aware of the danger of oversimplification, we nevertheless deduce a general pattern. Three main regions can be distinguished. The *first* of them is responsible for the MLCT transition with a maximum at about 500 nm. It is obvious

(24) Ballhausen, C. J.; Gray, H. B. *Molecular Orbital Theory*, W. A. Benjamin: New York, 1965.
(25) Calzaferri, G.; Forss, L. *Chem. Phys. Lett.* **1984**, *103*, 296.

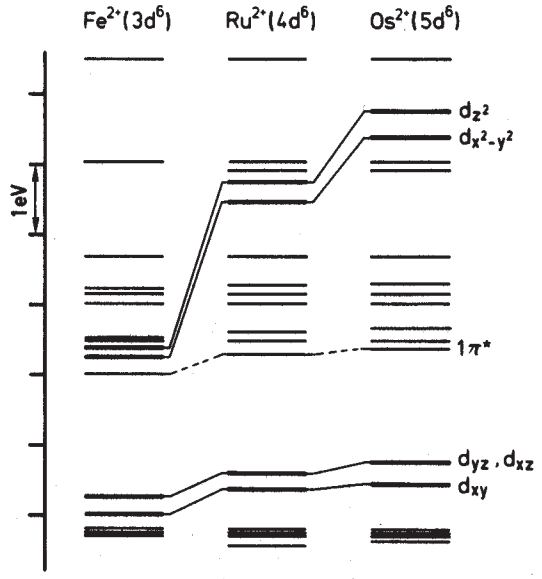

Figure 10. Correlation diagram of the Fe(II), Ru(II), and Os(II) H-ptpy complexes. The highest occupied d_{yz}, d_{xz}, and d_{xy} orbitals are each filled with two electrons.

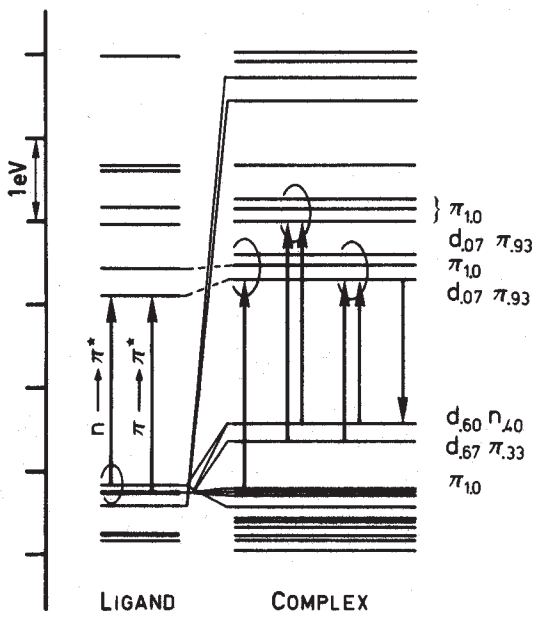

Figure 11. Comparison of the one-electron levels of the H-ptpy (left) with those of the $[Ru(H\text{-}ptpy)_2]^{2+}$ (right). Electronic transitions are indicated by arrows. The electronic configuration of important orbitals of the complex is indicated on the right side (one electron per orbital).

that not only one π^* orbital is involved. This is probably a reason for the complicated form of the absorption band that corresponds to this transition (Figure 2). The *second* region can still be described as MLCT transitions which appear, however, at about the same energy as the $\pi^* \leftarrow$ n in the free ligand, but with much higher intensity. In the *third* region finally we find the $\pi^* \leftarrow \pi$ transition. While they appear at nearly the same energy in the complex as in the ligand, a fact confirmed by the experiment, the lone pair orbitals interact with the central metal. That is why the $n\pi^*$ state has disappeared. The emission finally must clearly be attributed to a $d \leftarrow \pi^*$ transition. The two shoulders observed at intervals of about 1400 cm^{-1} are present in all the spectra of the investigated complexes and are ascribed to a number of aromatic C–C stretching vibrations.[26] These features indicate a relatively rigid structure of the ligand in the emitting state.[15c] As already explained, we have found that the ligand becomes planar and more rigid in the excited state (see Figure 8 and

(26) Hildebrandt, P.; Stockburger, M. *J. Phys. Chem.* **1984**, *88*, 5935.

SCHEME III

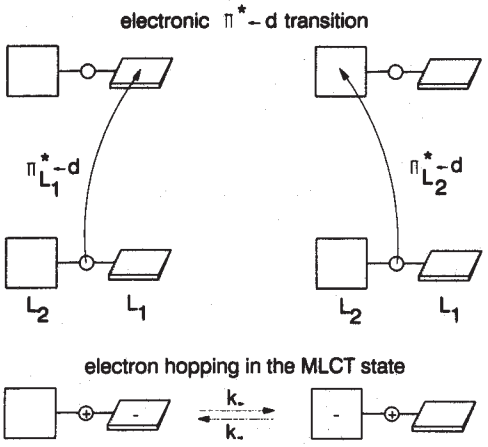

Scheme II). The situation in the MLCT state of the complex is similar. The minimum for the planar conformation is, however, more pronounced in the MLCT state than in the excited states of the free ligand due to the interaction with the d orbitals of the central atom. Another result that can be deduced from Figure 11 is that the visible part of the MLCT-state absorption spectrum should be similar to the absorption spectrum of the ligand radical anion.

What can we say with respect to the problem of localization versus delocalization of the electron in the excited state from the point of view of the molecular orbital description? Our arguments will be similar to those used in the description of binuclear complexes of the type $(L_1)_nM_1\text{–bridge–}M_2(L_2)_m$.[27]

The π^* orbitals involved in the MLCT state can be described as

$$\Pi^*_+ = c^+_M\Phi^+_M + c_L(\Phi_{\pi^*L_1} + \Phi_{\pi^*L_2}) \quad (11)$$

$$\Pi^*_- = c^-_M\Phi^-_M + c_L(\Phi_{\pi^*L_1} - \Phi_{\pi^*L_2}) \quad (12)$$

$\Phi^\pm_M$ are the d orbitals of the metal and $\Phi_{\pi^*L_1}$ and $\Phi_{\pi^*L_2}$ are π^* orbitals of the ligands. The ligands L_1 and L_2 are perpendicular to each other. As a consequence, $\Phi_{\pi^*L_1}$ and $\Phi_{\pi^*L_2}$ are perpendicular to each other and accidentally degenerate. Therefore, linear combinations $\Pi^*_+ \pm \Pi^*_-$ are valid molecular orbitals. Since the coefficients c^+_M and c^-_M are small or even zero (Figure 11), these "localized" orbitals can be approximated by the π^* orbitals $\Phi_{\pi^*L_1}$ and $\Phi_{\pi^*L_2}$, respectively:

$$\Psi^*_{L_1} = \frac{1}{2^{1/2}}(\Pi^*_+ + \Pi^*_-) \approx \Phi_{\pi^*L_1} \quad (13)$$

$$\Psi^*_{L_2} = \frac{1}{2^{1/2}}(\Pi^*_+ - \Pi^*_-) \approx \Phi_{\pi^*L_2} \quad (14)$$

This means that molecular orbitals localized on one of the two ligands present a valid wave function for describing the MLCT state and can be used as a basis for describing the electron-hopping mechanism illustrated in Scheme III. It will, however, never be possible to known whether during the electronic $\pi^* \leftarrow$ d transition the electron jumps directly to one of the ligands only. It is nevertheless interesting to investigate this possibility from a molecular orbital point of view. Let us look at the transition integral $\langle d|z|\Pi^*_\pm\rangle$. It can be expressed in terms of the localized wave function and split into two parts, each of them describing the transition to a single ligand:

$$\langle d|z|\Pi^*_\pm\rangle \approx \langle d|z|(\Phi_{\pi^*L_1} \pm \Phi_{\pi^*L_2})\rangle = \langle d|z|\Phi_{\pi^*L_1}\rangle \pm \langle d|z|\Phi_{\pi^*L_2}\rangle \quad (15)$$

As long as there is no external perturbation, the transition to both ligands is equally probable, and because of the accidental de-

(27) (a) Calzaferri, G. In *Photosynthetic Oxygen Evolution*; Metzner, H., Ed.; Academic Press: London, 1978; p 31. (b) Calzaferri, G. *Chimia* **1978**, *32*, 241.

generacy of the pair $\Pi^*_\pm$ we have a delocalized excited state. As soon as we allow even a small perturbation, the degeneracy is removed and hence the transition to one of the two ligands is favored. We end up with a localized state, the promoted electron staying on one ligand only. In dilute solution fluctuation of the solvent shell surrounding the complex can be regarded as cause for the perturbation. This means that in this case it is perfectly allowed to think in terms of a "localized excitation" (Scheme III). Does the electron stay on a single ligand or is it traveling between the two ligands? This question cannot be answered on the basis of a stationary-state theory because it involves time-dependent processes as, for example, the relaxation of the solvent shell. It seems, however, reasonable to think in terms of a double minimum potential.

Discussion

The problem of localization versus delocalization of the excitation energy is still a subject of controversy, even for $Ru(bpy)_3^{2+}$, the most popular ruthenium complex.[3a] In the first case, the excited electron is localized on one bipyridine ligand, whereas in the second case the excitation is delocalized over three equivalent ligands. While the delocalization argument seems to be favored by magnetic circular polarized luminescence,[28] the localization view is supported by many different techniques: low-temperature cyclic voltammetry and ESR,[29] luminescence polarization,[30] transient circular dichroism,[31b] time-resolved photoselection,[32] and time-resolved resonance Raman spectroscopy.[16a,17,18,20,31a] By comparing the transient excited-state absorption spectrum of the complex with the spectrum of the bipyridine anion, several authors reached the conclusion that the excited electron is localized on one bipyridine ligand.[16b,c,33] We have demonstrated recently that the visible bands of the excited state of a mixed-ligand complex, $[Ru(bpy)_2dppz]^{2+}$, have the same shape as those of the phenazine anion.[33a,b] This result suggests that the excited electron is localized on the phenazine part of the dipyridophenazine ligand. In $[Ru(bpy)_2dppz]^{2+}$ (dppz = dipyrido[3,2-*a*:2′,3′-*c*]phenazine), the three ligands are not equivalent, dppz being a stronger electron acceptor ligand than bpy. In the case of $[Ru(R\text{-}ptpy)_2]^{2+}$ where the two ligands are equivalent, the transient absorption spectra exhibit visible bands as observed for the $[Ru(bpy)_2dppz]^{2+}$ excited state. To examine the localization problem in the $[Ru(R\text{-}ptpy)_2]^{2+}$ complexes bearing two equivalent ligands, we have measured the electronic absorption spectra of the radical anions of the free ptpy ligands and we have compared them with the excited-state absorption spectra of the corresponding complexes. The similarity of the excited-state absorption spectra of the complexes with those of the ligand radical anions strengthens the idea that the excited electron is localized on a single ligand. This means that, in spite of the identity of the two ligands, the MLCT state has to be interpreted as $[(R\text{-}ptpy)Ru^{III}(R\text{-}ptpy^{\bullet-})]^{2+}$. This interpretation is supported by the reasoning that as long as there is no external perturbation, the electronic transition to both ligands is equally probable. As soon as we allow even a small perturbation, the transition to one of the two ligands is favored. The solvent shell surrounding the complex can be regarded as cause for the perturbation. The question whether the electron stays on a single ligand or whether it is traveling between the two ligands has probably to be answered in a similar way as reported for some mixed-ligand Ru(II) complexes.[34] It is reasonable to think in terms of a double minimum potential. The rate of hopping or tunneling from one well to the other is then a question of the characteristics of the barrier between them. The charge localization in the excited-state $[(R\text{-}ptpy)Ru^{III}(R\text{-}ptpy^{\bullet-})]^{2+}$ together with the structures makes it attractive to consider these compounds as select building units in supramolecular systems of dyad and triad types for directed photoinduced intramolecular charge transfer despite their low luminescence probability at room temperature. It has been shown recently[35] that an efficient photoinduced intramolecular electron transfer occurs in a dyad consisting of an Os^{II}R-ptpy complex covalently linked to methyl viologen. For similar reasons complexes with R-ptpy ligands are interesting candidates for conduction band $\leftarrow \pi^* \leftarrow$ d sensitization experiments.[5,38,39]

Acknowledgment. This work was initiated by a cooperation program (PICS) between CNRS France and the Swiss NF (Schweizerischer Nationalfonds zur Fördernung des wissenschaftlichen Forschung) during the time period 1987–1989. We would like to thank J. C. Brochon, Laboratoire pour l'Utilisation du Rayonnement Electromagnétique CNRS (LURE, Orsay), for his cooperation during the single photon counting experiments using synchrotron radiation, Ivo Kamber for his contributions and helpful discussions, and Annie Barat and René Bühler for their technical assistance.

(28) Ferguson, J.; Krausz, E. R. *Chem. Phys. Lett.* **1982**, *93*, 21.
(29) (a) Ohsawa, Y.; DeArmond, M. K.; Hanck, K. W.; Morris, D. E. *J. Am. Chem. Soc.* **1983**, *105*, 6522. (b) Morris, D. E.; Hanck, K. W.; De Armond, M. K. *J. Am. Chem. Soc.* **1983**, *105*, 3032. (c) Motten, A. G.; Hanck, K.; DeArmond, M. K. *Chem. Phys. Lett.* **1981**, *79*, 541.
(30) (a) Carlin, C. M.; DeArmond, M. K. *J. Am. Chem. Soc.* **1985**, *107*, 53. (b) Felix, F.; Ferguson, J.; Güdel, H. U.; Ludi, A. *J. Am. Chem. Soc.* **1980**, *102*, 4096. (c) Fujita, I.; Kobayashi, H. *Inorg. Chem.* **1973**, *12*, 2758.
(31) (a) Kumar, C. V.; Barton, J. K.; Gould, I. R.; Turro, N. J.; Van Houten, J. *Inorg. Chem.* **1988**, *27*, 648. (b) Gold, J. S.; Milder, S. J.; Lewis, J. W.; Kliger, D. S. *J. Am. Chem. Soc.* **1985**, *107*, 8285.
(32) (a) Myrick, M. L.; Blakley, R. L.; DeArmond, M. K. *J. Am. Chem. Soc.* **1987**, *109*, 2841. (b) Blakley, R. L.; Myrick, M. L.; DeArmond, M. K. *Inorg. Chem.* **1988**, *27*, 589.
(33) (a) Amouyal, E.; Homsi, A.; Chambron, J. C.; Sauvage, J.-P. *J. Chem. Soc., Dalton Trans.* **1990**, 1841. (b) Chambron, J. C.; Sauvage, J.-P.; Amouyal, E.; Koffi, P. *Nouv. J. Chim.* **1985**, *9*, 527. (c) Braterman, P. S.; Harriman, A.; Heath, G. A.; Yellowlees, L. J. *J. Chem. Soc., Dalton Trans.* **1983**, 1801.
(34) Yabe, Y.; Orman, L. K.; Anderson, D. R.; Yu, S.-C.; Xu, X.; Hopkins, J. B. *J. Phys. Chem.* **1990**, *94*, 7128.
(35) (a) Collin, J.-P.; Guillerez, S.; Sauvage, J.-P. *J. Chem. Soc., Chem. Commn.* **1989**, 776. (b) Amouyal, E.; Bahout, M. to be published.
(36) Elfring, W. H., Jr.; Crosby, G. A. *J. Am. Chem. Soc.* **1981**, *103*, 2683.
(37) Van Houten, J.; Watts, R. J. *J. Am. Chem. Soc.* **1975**, *97*, 3843.
(38) Amadelli, R.; Argazzi, R.; Bignozzi, C. A.; Scandola, F. *J. Am. Chem. Soc.* **1990**, *112*, 7099.
(39) Mohamad Nazeeruddin, K.; Liska, P.; Moser, J.; Vlachopoulos, N.; Grätzel, M. *Helv. Chim. Acta* **1990**, *73*, 1788.